Research Article | Vol. 32, No. 21 / 7 Oct 2024 / Optics Express 37127
Optics EXPRESS

Enhancing C+L-band transmission performance through OSNR flatting and link damage recovery algorithms

JING ZHOU,[1] JIANING LU,[1,*] ZHONGXU LIU,[1] QING WANG,[1] AND CHANGYUAN YU[1,2]

[1]Photonics Research Centre, Department of Electrical and Electronic Engineering, The Hong Kong Polytechnic University, Hung Hom, Kowloon, Hong Kong SAR, China
[2]The Hong Kong Polytechnic University Shenzhen Research Institute, Shenzhen 518057, China
*jianing.lu@connect.polyu.hk

Abstract: The rapid growth of data-intensive services has driven the need for high-capacity optical networks. C+L band optical communication systems have emerged as a potential solution by extending the operational bandwidth. However, the wider spectrum introduces significant stimulated Raman scattering (SRS) effects that impact signal power profile, Kerr nonlinearity, and amplified spontaneous emission (ASE) noise. To address these challenges, this paper proposes an optical power control strategy designed to achieve a flat optical signal-to-noise ratio (OSNR) across all transmitted channels, which is particularly effective in mitigating SRS effects in C+L band systems. Furthermore, a link damage recovery algorithm is developed to ensure system robustness against localized fiber degradations. Extensive simulations are conducted to compare the performance of the proposed strategy with the conventional flat launch power approach under single-span and multi-span transmission scenarios. The results demonstrate that the proposed strategy achieves a higher minimum generalized signal-to-noise ratio (GSNR), exhibits stronger resilience to link damage across a wide range of transmission conditions.

1. Introduction

The rapid development of online services, cloud computing, and the Internet of Things (IoT) is driving the demand for high-capacity optical networks [1]. To meet these capacity requirements while efficiently managing network infrastructures, operators are pursuing scalable and sustainable solutions that maximize the transmission capacity. Among the various strategies, C+L band optical communication system has emerged as a potential approach [2,3], which extends the operational bandwidth and capacity [4,5]. However, the broadening of the spectrum introduces considerable stimulated Raman scattering (SRS) effects [6,7], which skews the signal power profile and impacting the Kerr nonlinearity (NLI) as well as amplified spontaneous emission (ASE) noise [8,9]. To mitigate the impact of these effects on signal transmission, optical power control and generalized signal-to-noise ratio (GSNR) optimization have been investigated extensively for the ultra-wideband (UWB) transmission [10–12].

Optical power control is achieved by shaping the launch power profile (LPP) before the wavelength-division-multiplexing (WDM) signal is launched into the optical fiber [13,14]. Figure 1 illustrates two distinct C+L band power spectrum configurations by adjusting the EDFA operating parameters. Figure 1(a) depicts a flat power spectrum, where all channels operate at a specific power level. Figure 1(b) presents a pre-tilted power spectrum designed to eliminate some of the interference. Depending on the system physical layer and the objective function chosen, several strategies have been proposed for signal power control. Local optimization-global optimization (LOGO) algorithm performs power optimization for all channels with a uniform launch power, keeping a relatively low complexity [15,16]. Methods based on machine learning

#537942 https://doi.org/10.1364/OE.537942
Journal © 2024 Received 31 Jul 2024; revised 4 Sep 2024; accepted 18 Sep 2024; published 30 Sep 2024

Optics EXPRESS

(ML) and digital twins (DT) which enable more complex power control schemes also make a considerable progress [17–19]. Furthermore, some iteration-based algorithms are proposed to optimize the LPP of UWB system step-by-step [20,21]. Nevertheless, a simple and effective LPP optimization method which can be applied in practical complex system conditions is desired, so that the C+L transmission performance can have the ability to quickly recover from system degradation.

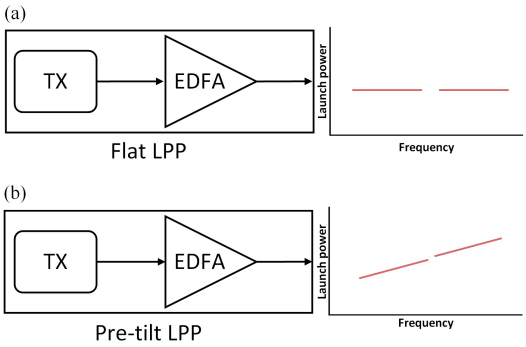

Fig. 1. The EDFA gain control strategies and the corresponding C+L band LPP example of (a) Flat LPP and (b) Pre-tilt LPP.

Optical signal to noise ratio (OSNR) and generalized SNR (GSNR) are both critical parameters in assessing the quality of transmission (QoT) [22–25]. Accurate QoT estimation can reduce the network design margin to improve the spectral efficiency [26–28]. OSNR is defined as the ratio of signal power to ASE noise power [29,30], while GSNR considers both linear and nonlinear noise factors, providing a more comprehensive assessment in ultra bandwidth system [9,22,31]. Analytical models, such as Gaussian noise (GN) models [6–8], use mathematical formulas to estimate the QoT, providing varying levels of accuracy depending on the complexity. Despite closed-form GN model in the presence of SRS has been proposed [8], the calculation complexity of GN model is still intolerant in practice and there has few devices can directly measure GSNR. This characteristic implies some challenges for algorithms that aim to optimize the GSNR distribution across all channels. In long-haul communication systems, it is difficult to optimize GSNR for each span, especially as future optical networks may likely adjust span lengths dynamically [19,32]. When faced with situations that require re-optimization of the LPP, such as occurring link damage, the inability to obtain real-time GSNR measurements or the time-consuming of GSNR estimation may not provide efficient and optimal solutions with the unknow physical parameters. Therefore, a flat LPP is commonly employed owing to its operational simplicity, straightforward monitoring, and the facilitation of swift recovery in the event of system localized link degradation. The flat LPP can be implemented easily by observation and adjusting EDFA parameters according to the optical channel monitor (OCM) which monitors the LPP after amplification in a real-time manner. Such strategy is efficient for C-band-only system but is not suitable for C+L band transmission where the SRS is severe. It is important to note that the channels with most power loss in high frequency part suffers a large amount of ASE due to higher gain for higher attenuation compensation.

To balance performance and simplicity, we propose an efficient power control strategy to achieve a flat OSNR profile, considering the significant SRS effect in C+L band systems. Since the NLI effect is strongest in the front part of the optical fiber where the optical power is higher and weakens after the power attenuates during propagation, it stands to reason that achieving the flattest OSNR spectra requires similar LPP for different span lengths, provided the fiber length exceeds a certain value, e.g., approximately 40 km. In long-haul fiber optic

Optics EXPRESS

communication systems, a single span of fiber typically exceeds 50 km. Therefore, we introduce a method to optimize a fixed LPP suitable for various fiber lengths to simplify operation in practical systems and develop a supporting algorithm to quick recover signal power from link damage, thereby improving robustness and reliability. We conduct a comprehensive comparison between our proposed method and the flat launch power approach under a large number of scenarios. The remainder of this paper is organized as follows: Section 2 provides a detailed description of the proposed OSNR flatting based power control strategy and the link damage recovery algorithm. Section 3 presents the simulation setup and the evaluation metrics used for performance assessment. Section 4 discusses the results obtained from the comparative analysis of the proposed method and the flat launch power approach, highlighting the advantages of our scheme in terms of QoT and resilience to link damage. Finally, Section 5 concludes the paper.

2. OSNR flatting based power control strategy and the link damage recovery algorithm

Figure 2 illustrates the considered configuration of the C+L band transmission system. The optical architecture encompasses the essential physical layer components, including transceivers, WDM, optical demultiplexer (Demux), booster amplifier (BA), inline amplifier (ILA), pre-amplifier (PA), OCM, and cascaded standard single model fiber (SSFM). The C+L band power spectrum is denoted as LPP_C and LPP_L. The ILAs and PAs are used to compensate the link loss and recover the power spectrum based on the power control strategy. The OCM is used to measure the amplified individual channel power amplitude, noted as LPP'_C and LPP'_L.

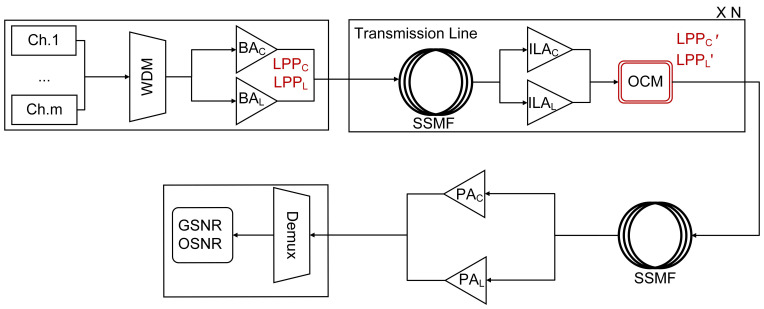

Fig. 2. The optical transmission architecture for C+L band system.

As the LP flattening strategy is one of the most common power control strategies in practice, we apply it for performance comparison. In this strategy, the LP is scanned from 2 dBm to 5 dBm, and the gain and slope of the PAs are adjusted to restore a flat power spectrum based on link physical knowledge and OCM information.

2.1. OSNR flatting optical power control strategy

A flowchart for the power control strategy is shown in Fig. 3 and can be divided into several steps:

1. We start by setting the power of the rightmost channel in the L-band (LP_L) and the leftmost channel in the C-band (LP_C) at 2 dBm, noted as LP_C=LP_L= LP_i = 2 dBm.

2. We scan the tilts of C and L band from -4dB to 0dB, noted as $tilt_{C,i,m}$, $tilt_{L,i,n}$. The corresponding LPP noted as $LPP_{C,i,m}$ and $LPP_{L,i,n}$.

3. We perform link transmission simulation. The gain of PA_C and PA_L is equal to the fiber link loss. The tilts of PA_C and PA_L are scanned from -4dB to 0dB. The output power of the PAs is defined as $LPP'_{C,i,m}$ and $LPP'_{L,i,n}$. The tilt value of the PA_C is evaluated and determined when $LPP'_{C,i,m}$ equals $LPP_{C,i,m}$. The tilt value of PA_L is determined by the same method.

Optics EXPRESS

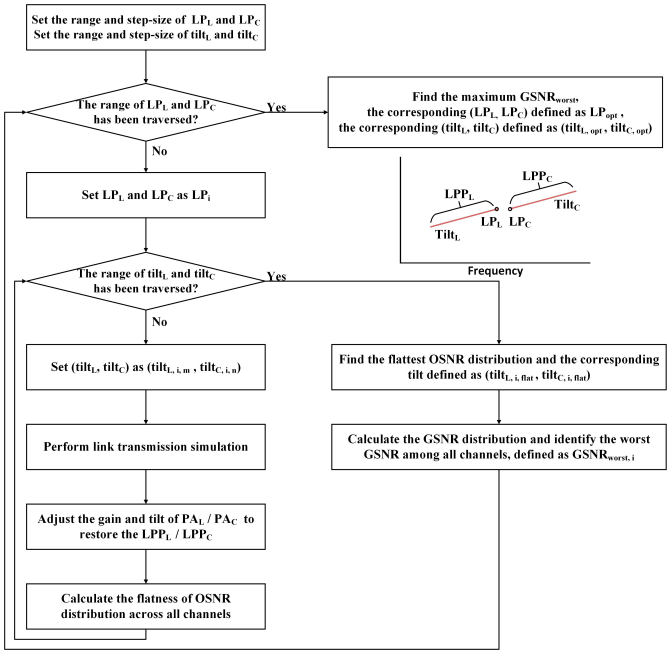

Fig. 3. Flowchart of the proposed optical power control strategy.

4. The NLI and ASE noise are calculated based on the PA_C and PA_L settings and the knowledge of physical layer. We estimate the OSNR and calculate the corresponding flatness across all channels. The degree of OSNR flatness is represented by its Standard Deviation:

$$\sigma_i = \sqrt{\frac{\sum(x_i - \mu)^2}{N}}. \tag{1}$$

5. Repeat the step 2-4 until the tilt range of C- and L-band has been traversed. Compare all the OSNR flatting results to find the flattest OSNR distribution, denoted as $OSNR_{i,flat}$. Its corresponding tilt configuration is denoted as ($tilt_{C,i,flat}$, $tilt_{L,i,flat}$). Estimate the corresponding GSNR based on the closed-from GN model which takes SRS into account [33], denoted as $GSNR_i$. The GSNR of the worst channel is noted as $GSNR_{i,worst}$.

6. We identify the maximum value among all the $GSNR_{i,worst}$ noted as $GSNR_{worst}$. The corresponding gain and tilt configurations of LPP are noted as LP_{opt}, $tilt_{C,opt}$, and $tilt_{L,opt}$

It is worth mentioning that our proposed method requires running the GN model only after determining the flattest OSNR power profile for the central channel. In contrast, traditional GSNR optimization typically involves extensive GN model calculations. As a result, our approach is simpler and more efficient.

2.2. Link damage recovery algorithm

Typically, the network operator aims to maintain the optimized power spectrum as much as possible during signal transmission. However, optical fiber link is susceptible to various types of damages that can cause significant power spectrum degradation. Degradation in optical fibers primarily affects signal quality by inducing power losses and causing signal distortion. Therefore, rapid and effective recovery algorithm are essential to maintain optimal network performance.

We propose a supporting link damage recovery algorithm based on our proposed power control strategy. The algorithm is capable of compensating for power degradation and rapidly recovering

Optics EXPRESS

the optimized LPP by adjusting the gain and tilt of PAs based on real-time LPP monitored by OCM. We use an OCM to continuously monitor the center channel power levels of the C- and L-bands (LP_C, LP_L). By comparing the monitored power levels with the optimized center power amplitude ($LP_{C,opt}$, $LP_{L,opt}$), if the monitored value exceeds the expected value by more than 0.5 dB, the PAs will make corresponding rapid adjustments to recovery the optimized LPP. The diagram is shown in Fig. 4, and the algorithm works in two main steps:

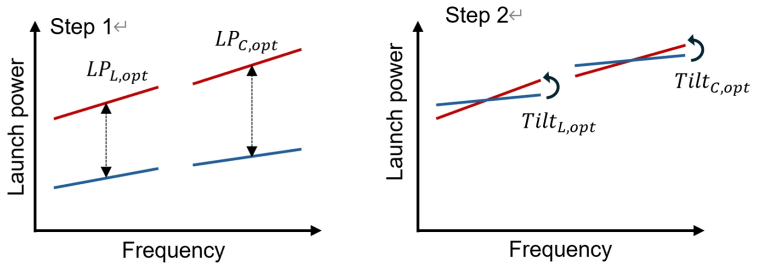

Fig. 4. The diagram of the proposed link damage recovery algorithm.

Step 1: The PAs adjust the gain value to bring the center channel power levels back to their values ($LP_{C,opt}$, $LP_{L,opt}$) in the optimized LPP.

Step 2: The tilt of the PAs is iteratively scanned until the adjusted power profile is equal to the optimized power profile, which is achieved when mean squared error of all channel powers between the adjusted power profile and optimized power profile is less than 0.1 dB.

The proposed strategy is designed for fully-loaded C+L systems, which have the ability to automatically fill ASE noise channels to maintain a fully loaded condition. Nevertheless, for those partial loading conditions, the strategy still work as long as the spectrum remains relatively continuous or only a small portion of the channels are lost.

Overall, this proposed iterative power control strategy enables the strategy to converge on the LPP control and PA settings that optimize the received OSNR flatness. Subsequent simulations will demonstrate the improvements in system performance brought by our proposed method.

3. Simulation setup and LPP optimization

At the transmitter side, each channel is assumed a rectangular spectrum, employing ideal Nyquist shaping with zero roll-off factor. The WDM comb consists of 128 channels spanning the C and L bands, from 186.1125 THz to 196.0875 THz, with a channel spacing of 75 GHz and a baud rate of 67 Gbaud. To mitigate potential interference between the C and L bands, a guard band of five channels separates these two spectral regions. The noise figures (NF) for the C-band and L-band are 4.5 and 6, respectively. Although the NF is frequency-dependent and related to the amplifier gain value, we approximate it as flat here. Some works are focus on reducing the uncertainty of the NF, and some open-source data regarding the relationship between EDFA gain and NF are published [34].

Based on the proposed OSNR flatting strategy, we optimize the LPP through two steps: (1) the transmission line use an 80 km SSMF and scan the center frequency power (LP_C, LP_L) from 2-5 dBm, as depicted in Fig. 5(a). Then, the tilt of the C and L bands is individually adjusted from -4 dB to 0 dB with a step size of 0.1 dB, respectively. Figure 5(b) illustrates the process of varying the power profile. All possible LPPs are input into the system, and their corresponding OSNR distribution are calculated.The examples of OSNR are shown in Fig. 5(c).The flatness of each OSNR distribution is evaluated to identify the flattest one, followed by the calculation of its corresponding GSNR distribution. The result is shown in Fig. 5(d). Figure 5(e) shows the relationship between the center frequency power and the corresponding worst GSNR for the two

Optics EXPRESS

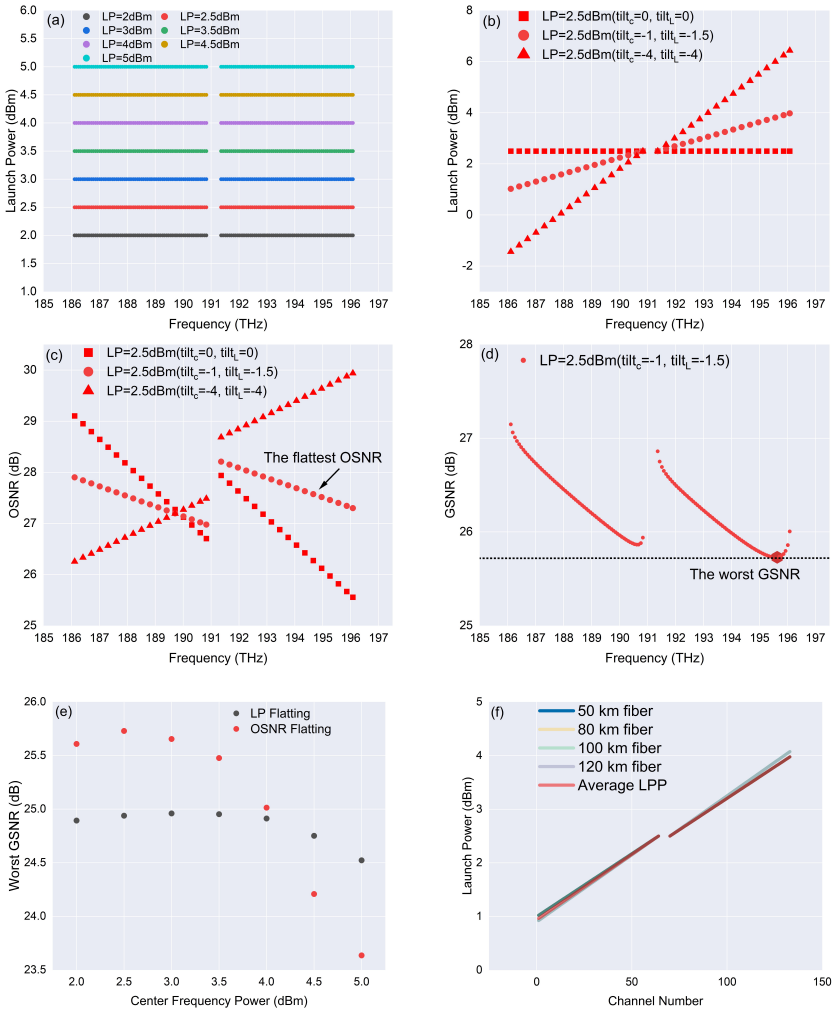

Fig. 5. (a) The range of center frequency power. (b) Examples to illustrate the variation in LPP distribution across the frequency spectrum. (c) Examples to illustrate the variation in OSNR distribution. (d) The estimated GSNR using the LPP that produces the flattest OSNR. (e) The results of LP flatting and OSNR flatting strategies on worst GSNR across center frequency power value. (f) The optimal LPPs for different fiber lengths using the OSNR flattening strategy, along with the average LPP.

strategies. To make sure that each strategy operates at its optimal working point, 2.5 dBm is set as the central power for our proposed strategy, and 3 dBm is set for the LP flatting strategy. (2) We fix the (LP_C, LP_L) at 2.5 dBm and the fiber length is varies among 50 km, 80 km, 100 km, and 120 km, which are most typical values for practical systems. We obtain the corresponding optimal tilt ($tilt_{C,opt}$, $tilt_{L,opt}$) for each scenario by applying our proposed method. The results are depicted in Fig. 5(f), and we calculate the average LPP among all link options (red line). This average LPP is noted as optimal LPP and it is fixed for the C+L transmission to provide a robust, near-optimal solution across various link conditions, balancing performance, and practicality for network deployment. All transceivers and regeneration station use this power profile for fiber lengths up to 120 km. It should be noticed that this optimal LPP is calculated based on the specific channel arrangement, baud rate, and amplifier gain and NF. Different optimizations

Optics EXPRESS

can be performed for different systems. We will demonstrate the effectiveness of this approach through a series of scenarios.

Once the optimal launch power profile is determined, it remains constant for each transmitter location and will be adjusted by the amplifiers before each span to match the optimized LPP.

4. Results and discussions

4.1. Comparison of two strategies under single-span transmission

We first investigate two strategies under single span with 50 km, 80 km, 100 km, and 120 km fiber lengths in the single-span transmission system, with the configuration depicted in Fig. 2. The link is intact without any degradation. At the receiver side, we calculate the ASE noise and leverage the GN model to estimate the nonlinear noise. The results of OSNR and GSNR are presented in Fig. 6.

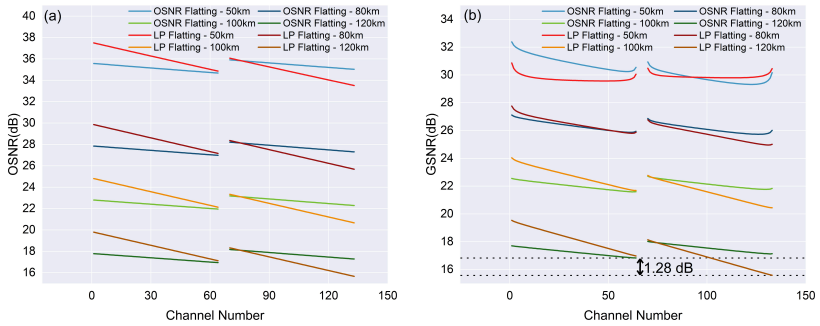

Fig. 6. The performance of (a) OSNR and (b) GSNR for two strategies in a single-span fiber optic system across different channel numbers.

Referring to Fig. 6(a), the proposed OSNR flatting strategy achieves a remarkably flat received OSNR distribution across the entire bandwidth. While the system using LP flatting strategy has a relatively sloped OSNR distribution. On the other hand, although the LPP is optimized for a OSNR flatting distribution, the received GSNR demonstrates a similar trend. In Fig. 6(b), beyond 50 km, the OSNR flatting strategy yields a significantly flatter and elevated GSNR profile compared with that using LP flatting strategy, particularly in the C-band. The worst GSNR also experiences a substantial enhancement. Under a 120 km fiber link, the worst GSNR of the two methods differs by 1.28 dB. That gap indicates that our method effectively mitigates the risk of BER degradation by maintaining a flat and relatively high GSNR, thereby improving transmission performance and reliability.

In this part, we assess the robustness to link degradations of the OSNR flatting strategy and LP flatting strategy under the condition of an 80 km single-span fiber. A loss of 1 dB is introduced at the midpoint of the span (40 km). This investigation is conducted without the implementation of any compensatory mechanisms, to directly observe the impacts of link damage on the OSNR and the GSNR distribution. The data presented in Fig. 7 indicates the performance degradation with both strategies. As shown in the Figs. 7(a),(b), the OSNR in the L-band is higher with the LP flattening strategy compared to our proposed method, while in the C-band the OSNR is lower than that of our approach. Moreover, our strategy yields a flatter OSNR distribution and a higher worst-case OSNR. The OSNR of the worst channel has improved by 1.17 dB. For the GSNR results, while some channels in the L-band show higher GSNR under the LP flattening strategy, our approach achieves higher GSNR in the whole C-band, and the worst-case GSNR is nearly 1.4 dB higher. We also present the OSNR and GSNR for the LP flattening strategy and

Optics EXPRESS

the OSNR flattening strategy under a 1 dB loss condition, similar performance trend are shown in Figs. 7(c),(d).

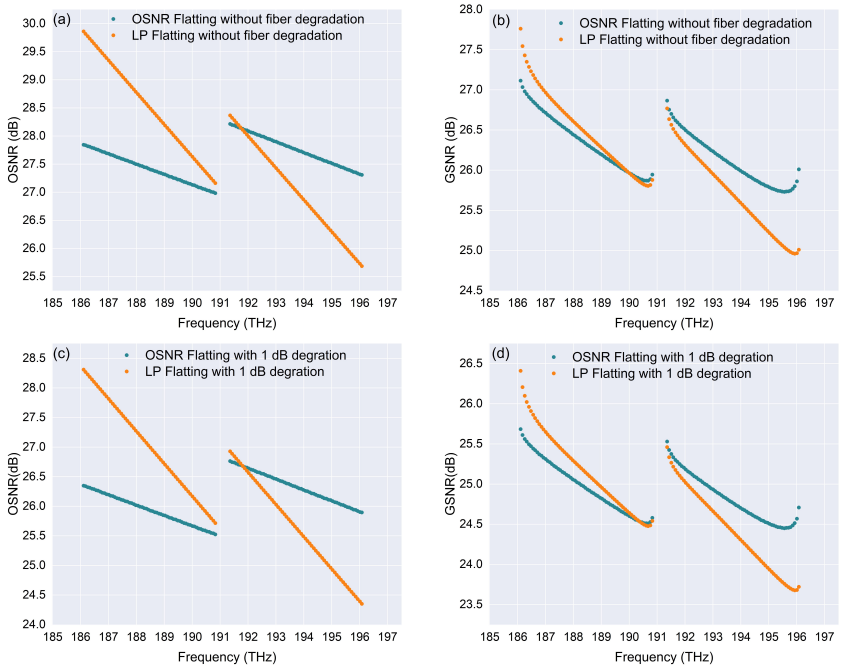

Fig. 7. (a) OSNR distribution without fiber degradation. (b) GSNR distribution without fiber degradation. (c) OSNR distribution with 1 dB fiber degradation. (d) GSNR distribution with 1 dB fiber degradation.

Figure 8 demonstrates the performance of the link damage recovery algorithm based on two optimization strategies under a single-span 80 km link with a 1 dB localized degradation at 10 km, 40 km, and 70 km from the transmitter. Figure 8(a) presents the simulation results of the OSNR flatting strategy after LPP compensation. It illustrates that damage occurring at the 10 km point results in GSNR decline of 0.3 dB in the outermost channels of the L-band. This is primarily due to a reduction in overall power, which weakens the effects of SRS, thereby the power pumped from the C-band to the L-band decreases [9]. Consequently, there is a slight increase for the C-band signal while the L-band signal experiences a reduction. However, the worst-case GSNR shows little change. For fiber degradation at 40 km and 70 km, the GSNR at the receiver-side shows almost no change. This stability is primarily due to once the signal has been transmitted to the mid-span, the signal power is relatively low caused by fiber loss, and additional fiber losses are unlikely to significantly affect the distribution of SRS [33]. Resolved the potential new power tilt caused by SRS due to degradation, the impact of link damage is effectively controlled by the pre-tilted scheme.

Figure 8(b) presents the performance of the LP flatting strategy after LPP compensation. It is evident that the overall GSNR at the receiver end becomes increasingly skewed as the localized distance of degradation increases. The lowest GSNR decreases from 24.15 dB to 23.73 dB, reducing approximately 0.42 dB. This phenomenon occurs because a flat LPP fails to counteract the effects of SRS. Moreover, degradation occurring later along the span means a greater SRS impact, leading to more power pumping from C-band to L-band. Consequently, a higher compensatory gain is required, which in turn increases the ASE noise, further diminishing the GSNR.

Optics EXPRESS

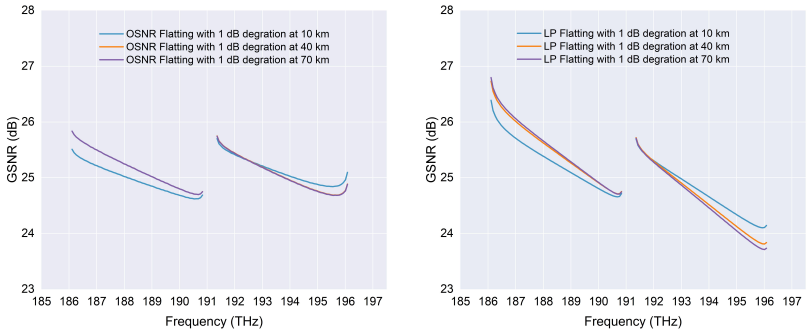

Fig. 8. The GSNR performance after applying link damage recovery algorithm under (a) OSNR Flatting and (b) LP Flatting Strategies with 1dB localized degradation in an 80 km single-span optical link.

Figure 9 illustrates the evolution of the minimum GSNR as the location of the localized impairment shifts along the transmission link. The results reveal a notable trend: the detrimental impact on the minimum GSNR becomes increasingly significant as the impairment occurs closer to the transmitter-side. Notably, the proposed strategy consistently outperforms the conventional LP flatting strategy. The OSNR flatting strategy maintain a higher minimum GSNR across all scenarios when impairments occur at different distances along the span. In contrast, the LP flatting strategy shows a marked decline in GSNR, particularly as the impairment moves closer to the receiver-side.

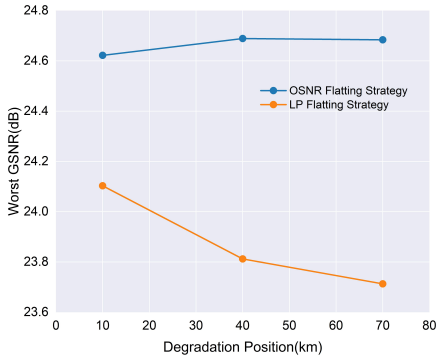

Fig. 9. The worst GSNR of OSNR flatting and LP flatting strategies across varying degradation positions.

4.2. Comparison of two strategies under multi-span transmission

To comprehensively demonstrate the effects of link degradation and proposed supporting compensation algorithm, we conduct signal transmission simulations over six spans, with identical length of 80 km. In these simulations, 1 to 3 localized link degradations ranging from 1 dB to 3 dB are introduced randomly at any point along the spans. Figure 10 presents the statistical distribution of the worst-case GSNR for 10,000 times simulation results. All conditions are not applying the supporting compensation algorithm. Across 10,000 random scenarios, it is evident that the proposed strategy outperforms the LP flatting strategy by a notable GSNR margin of 0.93 dB. This improved stability offers a significant advantage for multi-span transmission, ensuring

Optics EXPRESS

more reliable data transmission over fiber-optic links subject to random degradations. The OSNR flatting strategy offers higher stability under complex link degradation conditions.

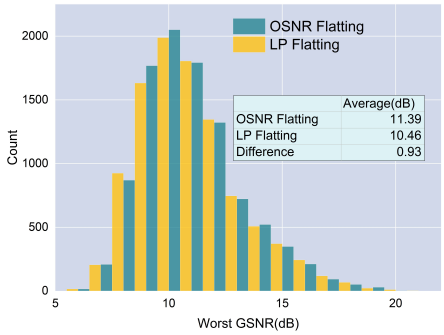

Fig. 10. Statistical distribution of worst-case GSNR for OSNR flatting and LP flatting strategies in a multi-span system with randomly generated 1-3 degradations, each within the range of 1 to 3 dB.

Figures 11(a)–(c) presents the performance of the two strategies after applying link damage recovery algorithm under conditions of 1, 2, and 3 link degradation, respectively. The link damage recovery algorithm for OSNR flatting strategy has been previously described. The link damage recovery scheme of LP flatting strategy is directly increasing the PA gain without adjusting the tilt. Comparing the data from Fig. 10 and Fig. 11, it is clear that compensation significantly improves the average worst-case GSNR for both strategies. For OSNR flatting, the average GSNR increases from 11.39 dB without compensation to a range of 15.12-15.52 dB with compensation. Similarly, for LP flatting, the average GSNR increases from 10.46 dB without compensation to a range of 14.32-14.76 dB with compensation. These results indicate that the OSNR flatting strategy consistently provides better GSNR performance compared to the LP flatting strategy, particularly when compensation is applied. This demonstrates higher stability and improved performance of the OSNR flatting strategy under complex link degradation conditions.

We conduct more complex transmission simulations under a random number of spans ranging from 1 to 6, where the fiber length of each span is randomly selected from 50, 80, 100, or 120 km. Two strategies are simulated under both with-degradation and without-degradation conditions, yielding a comprehensive set of four comparative cases. The degradations are varied between 1 dB to 3 dB and localized at arbitrary position along the span. Through 10,000 independent simulations, the worst GSNR distribution is demonstrated in Fig. 12. We avoid applying link damage recovery to illustrate the worst-case performance of the two schemes when the link degradation occurs.

Under non-degraded conditions, the OSNR flatting strategy (represented by the black line) consistently outperforms the LP flatting strategy (represented by the blue line) by nearly 1 dB, indicating its superior capability in optimizing signal quality. Under random degradation conditions, the average worst GSNR of proposed strategy is 11.37 dB, while the average worst GSNR of LP flatting strategy is 10.4 dB, showing an increase of 0.97 dB. The results clearly demonstrate the superior performance over the LP flatting strategy across all scenarios.

Optics EXPRESS

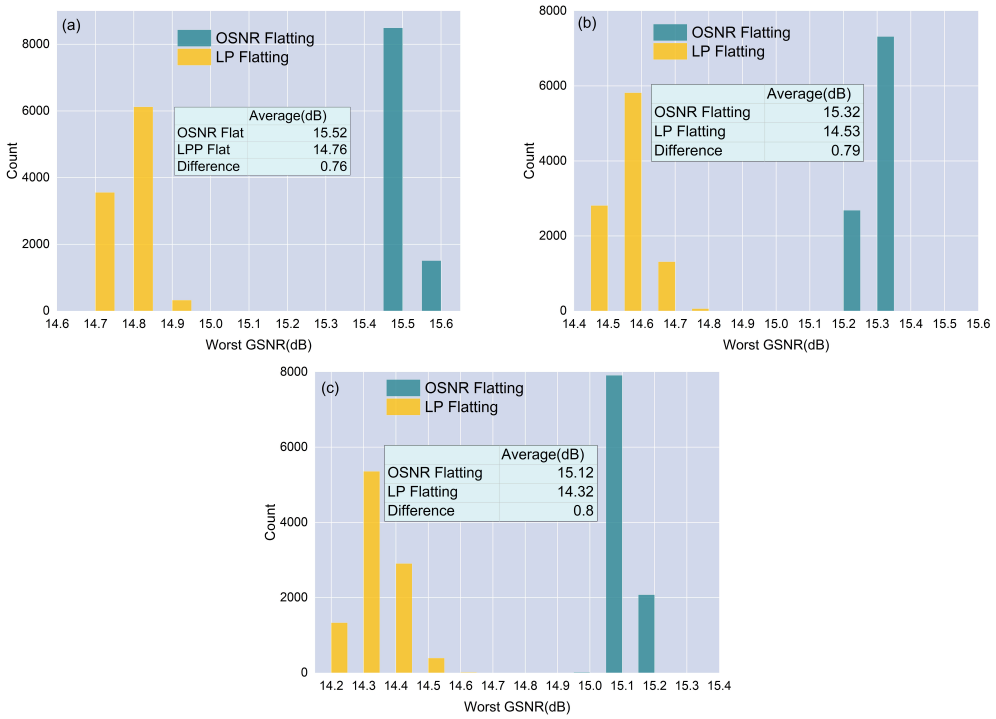

Fig. 11. Statistical distribution of the worst-case GSNR for OSNR flatting and LP flatting strategies in a multi-span system with (a) 1, (b) 2, (c) 3 randomized link degradation after applying link damage recovery algorithm, with each degradation within the range of 1 to 3 dB.

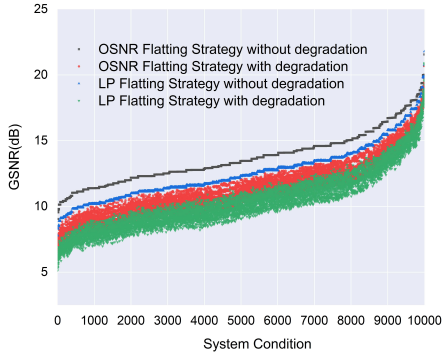

Fig. 12. The worst GSNR statistical distribution of OSNR flatting and LP Flatting strategies across varying transmission system conditions.

5. Conclusion

In this paper, we introduce a novel power control strategy to achieve a flat OSNR distribution across all channels at the receiver side for C+L band transmission systems. The proposed strategy has the advantage of straightforward computation and capable to effectively mitigating the impact of SRS. The performance is comprehensively investigated comparing with the LP flatting strategy under diverse system conditions. The results demonstrate the significantly improvement for the GSNR. We also propose a corresponding recovery algorithm to fast recovery the optimized

Optics EXPRESS

LPP in case of occurring random link degradation. Above all, the proposed strategy can be an important and helpful supplement for power control in practical C + L band long-haul fiber optical communication systems.

Funding. Hong Kong Government (GRF Project No. 15209321).

Disclosures. The authors declare no conflicts of interest.

Data availability. Data underlying the results presented in this paper are not publicly available at this time but may be obtained from the author upon reasonable request.

References

1. T. Barnett, S. Jain, U. Andra, *et al.*, "Cisco visual networking index (vni) complete forecast update, 2017–2022," Americas/EMEAR Cisco Knowledge Network (CKN) Presentation 1, 1 (2018).
2. S. Okamoto, K. Minoguchi, and F. Hamaoka, "A study on the effect of ultra-wide band WDM on optical transmission systems," J. Lightwave Technol. **38**(5), 1061–1070 (2020).
3. M. Cantono, R. Schmogrow, and M. Newland, "Opportunities and challenges of C+L transmission systems," J. Lightwave Technol. **38**(5), 1050–1060 (2020).
4. J. X. Cai, H. G. Batshon, M. V. Mazurczyk, *et al.*, "94.9 Tb/s single mode capacity demonstration over 1,900 km with C+L EDFAs and coded modulation," in *European Conference on Optical Communication* (2018), pp. 1–3.
5. J. K. Fischer, M. Cantono, V. Curri, *et al.*, "Maximizing the capacity of installed optical fiber infrastructure via wideband transmission," in *20th International Conference on Transparent Optical Networks* (2018), pp. 1–4.
6. D. Semrau, R. I. Killey, and P. Bayvel, "The Gaussian noise model in the presence of inter-channel stimulated Raman scattering," J. Lightwave Technol. **36**(14), 3046–3055 (2018).
7. P. Poggiolini, G. Bosco, and A. Carena, "The GN-model of fiber non-linear propagation and its applications," J. Lightwave Technol. **32**(4), 694–721 (2014).
8. I. Roberts, J. M. Kahn, J. Harley, *et al.*, "Channel power optimization of WDM systems following Gaussian noise nonlinearity model in presence of stimulated Raman scattering," J. Lightwave Technol. **35**(23), 5237–5249 (2017).
9. F. Hamaoka, M. Nakamura, S. Okamoto, *et al.*, "Ultra-wideband WDM transmission in S, C, and L-bands using signal power optimization scheme," J. Lightwave Technol. **PP**, 1 (2019).
10. H. Buglia, E. Sillekens, and A. Vasylchenkova, "On the impact of launch power optimization and transceiver noise on the performance of ultra-wideband transmission systems [invited]," J. Opt. Commun. Netw. **14**(5), B11–B21 (2022).
11. B. Correia, R. Sadeghi, and E. Virgillito, "Power control strategies and network performance assessment for C+L+S multiband optical transport," J. Opt. Commun. Netw. **13**(7), 147–157 (2021).
12. X. Yang, A. Ferrari, N. Morette, *et al.*, "Experimental impact of power re-optimization in a mesh network," in *European Conference on Optical Communication* (2022), pp. 1–4.
13. M. P. Yankov, U. C. de Moura, and F. D. Ros, "Power evolution modeling and optimization of fiber optic communication systems with EDFA repeaters," J. Lightwave Technol. **39**(10), 3154–3161 (2021).
14. E. d. A. Barboza, A. A. B. da Silva, and J. C. P. Filho, "Optical amplifier response estimation considering non-flat input signals characterization based on artificial neural networks," J. Lightwave Technol. **39**(1), 208–215 (2021).
15. P. Poggiolini, G. Bosco, A. Carena, *et al.*, "The LOGON strategy for low-complexity control plane implementation in new-generation flexible networks," in *Optical Fiber Communication Conference and Exposition and the National Fiber Optic Engineers Conference* (2013), pp. 1–3.
16. G. Borraccini, S. Straullu, and A. D'Amico, "Local and global optimization methods for optical line control based on quality of transmission," J. Opt. Commun. Netw. **16**(5), B60–B70 (2024).
17. Y. Zhang, X. Pang, and Y. Song, "Optical power control for GSNR optimization based on C+L-band digital twin systems," J. Lightwave Technol. **42**(1), 95–105 (2024).
18. D. Wang, Z. Zhang, and M. Zhang, "The role of digital twin in optical communication: Fault management, hardware configuration, and transmission simulation," IEEE Commun. Mag. **59**(1), 133–139 (2021).
19. Y. Zhang, M. Zhang, and Y. Song, "Building a digital twin for large-scale and dynamic C+L-band optical networks," J. Opt. Commun. Netw. **15**(12), 985–998 (2023).
20. Y. Song, Q. Fan, and C. Lu, "Efficient three-step amplifier configuration algorithm for dynamic C+L-band links in presence of stimulated Raman scattering," J. Lightwave Technol. **41**(5), 1445–1453 (2023).
21. I. Roberts, J. M. Kahn, and D. Boertjes, "Convex channel power optimization in nonlinear WDM systems using Gaussian noise model," J. Lightwave Technol. **34**(13), 3212–3222 (2016).
22. N. Morette, H. Hafermann, Y. Frignac, *et al.*, "Machine learning enhancement of a digital twin for wavelength division multiplexing network performance prediction leveraging quality of transmission parameter refinement," J. Opt. Commun. Netw. **15**(6), 333–343 (2023).
23. Y. Pointurier, "Machine learning techniques for quality of transmission estimation in optical networks," J. Opt. Commun. Netw. **13**(4), B60–B71 (2021).
24. A. S. Kashi, Q. Zhuge, J. C. Cartledge, *et al.*, "Fiber nonlinear noise-to-signal ratio monitoring using artificial neural networks," in *European Conference on Optical Communication* (2017), pp. 1–3.
25. D. Wang, M. Zhang, and Z. Li, "Modulation format recognition and OSNR estimation using CNN-based deep learning," IEEE Photonics Technol. Lett. **29**(19), 1667–1670 (2017).

Optics EXPRESS

26. J.-L. Augé, "Can we use flexible transponders to reduce margins?" in *Optical Fiber Communication Conference and Exposition and the National Fiber Optic Engineers Conference* (2013), pp. 1–3.
27. E. Ehsani, H. Beyranvand, and J. Salehi, "Routing, spectrum and modulation level assignment, and scheduling in survivable elastic optical networks supporting multi-class traffic," J. Lightwave Technol. **PP**, 1 (2018).
28. E. Seve, J. Pesic, and C. Delezoide, "Learning process for reducing uncertainties on network parameters and design margins," J. Opt. Commun. Netw. **10**(2), A298–A306 (2018).
29. F. N. Khan, K. Zhong, and X. Zhou, "Joint OSNR monitoring and modulation format identification in digital coherent receivers using deep neural networks," Opt. Express **25**(15), 17767–17776 (2017).
30. A. D'Amico, E. London, E. Virgillito, *et al.*, "Quality of transmission estimation for planning of disaggregated optical networks," in *International Conference on Optical Network Design and Modeling* (2020), pp. 1–3.
31. D. Semrau, R. I. Killey, and P. Bayvel, "A closed-form approximation of the Gaussian noise model in the presence of inter-channel stimulated Raman scattering," J. Lightwave Technol. **37**(9), 1924–1936 (2019).
32. J. Zhou, J. Lu, C. Lu, *et al.*, "Analysis of capacity upgrading in l-band using power control strategy," in *Region 10 Conference* (IEEE, 2022), pp. 1–4.
33. Y. Pointurier, "Design of low-margin optical networks," J. Opt. Commun. Netw. **9**(1), A9–A17 (2017).
34. Z. Zhai, L. Dou, and Y. He, "Open-source data for qot estimation in optical networks from alibaba," J. Opt. Commun. Netw. **16**(1), 1–3 (2024).